Bulletin of Geosciences, Vol. 79, No. 4, 205–219, 2004
© Czech Geological Survey, ISSN 1214-1119

Zircon Pb-Pb and U-Pb systematics of TTG rocks in the Congo Craton: Constraints on crust formation, magmatism, and Pan-African lead loss

Cosmas Kongnyuy Shang [1, 2] – Wolfgang Siebel [1] – Muharrem Satir [1] – Fukun Chen [1, 3] – Joseph Ondoua Mvondo [2]*

[1] University of Tübingen, Department of Earth Sciences, D-72074, Germany. E-mail: cosmas@uni-tuebingen.de; wolfgang.siebel@uni-tuebingen.de.
[2] University of Yaounde I, Department of Earth Sciences, BP 812, Yaounde, Cameroon.
[3] Chinese Academy of Sciences, Institute of Geology and Geophysics, P.O. Box 9825, Beijing 100029, China. E-mail: fukun-chen@mail.igcas.ac.cn
*Corresponding author

Abstract. Tonalite-Trondhjemite-Granodiorite (TTG) intrusions in the Sangmelima region of the Ntem complex represent a major Archean accretion event in the Congo craton. These intrusions are characterized by calc-alkaline rocks of a charnockitic suite, a tonalitic suite, and granodiorites. Zircons from these rock types have high Th/U ratios. Their internal structure is characterized by oscillatory zoning of magmatic origin, with recrystallization overprints and relict cores. Zircon $^{207}Pb/^{206}Pb$ evaporation data are interpreted to indicate crystallization ages, inheritance, and later disturbance. $^{207}Pb/^{206}Pb$ zircon data point to a Mesoarchaean emplacement between 2800 and 2900 Ma, with the intrusion of rocks of the charnockitic suite being followed by granodiorites and the tonalitic suite. While older age data (> 2900 Ma) suggest the existence of an older crust prior to TTG emplacement, younger data (< 2800 Ma) are strong indications for Pb loss due to post-emplacement reworking of the TTG suite. However, high proportions of a common Pb component suggest Pb gain. The Pb-Pb systematics of zircon therefore suggests a complex post-magmatic history for the Sangmelima TTG. Conventional U-Pb zircon dating confirms this observation, suggesting that the Pan-African tectonothermal event was the principal cause of the disturbance of zircon Pb-Pb systematics in the Sangmelima region.

Key words: Ntem complex, Congo craton, TTG suite, Pb-Pb evaporation, U-Pb zircon dating, Pan-African, Archaean

Introduction and objective of study

Tonalite-Trondhjemite-Granodiorite (TTG) suites appear to be the dominant rock types in most Archaean cratonic terrains. Constraints on their intrusive timing are therefore essential for comprehending the development of old continental crust. Several geochronological methods and techniques of investigation have been used to determine the timing of TTG magmatism in vast cratonic areas such as the Baltic shield and the Pilbara craton of Western Australia, while independent time constraints on their geologic and geodynamic development have been suggested. Some of these investigative methods also suggest various geological-geochemical pre-syn-post emplacement imprints in these basement complexes. So far, fairly little is known about the Congo craton. The northwestern part of this craton in southern Cameroon is known as the Ntem complex (e.g., Clifford and Class 1970, Cahen et al. 1976, Bessoles and Trompette 1980). Although the Ntem complex has been the subject of investigation since colonial times, most study has been based on recent geochemical characterization (e.g., Nédélec et al. 1990, SW Cameroon project piloted by BRGM, 1975–86), while vast areas of this complex have received little or no geochronological identification. However, some isolated works (e.g., Delhal and Ledent 1975, Lasserre and Soba 1976, Nzenti et al. 1988, Toteu et al. 1994, Tchameni 1997, Tchameni et al. 2000, 2001, Shang et al. 2001a) do point to the Archaean as the principal period of the formation of the Ntem cratonic crust. In the present paper, we present new single zircon Pb-Pb evaporation and conventional U-Pb data from the Sangmelima calc-alkaline TTG suite of the Ntem complex, which is largely composed of charnockitic and tonalitic members as well as granodiorites of indisputable igneous origin. Our data provide some insight into the complex crystallization and post-magmatic evolutionary history of these rocks.

Geological setting and composition of the rocks

The Ntem complex comprises the northwestern part of the Archaean Congo craton in Central Africa (e.g., Clifford and Class 1970, Cahen et al. 1976, Bessoles and Trompette 1980), and is very well exposed in southern Cameroon (e.g., Maurizot et al. 1986, Goodwin 1991; Fig. 1). It is limited in the north by a major thrust that marks the contact with the Pan-African orogenic belt, and is composed of various rock types, with those of the TTG suite constituting the greater part (e.g., Nédélec et al. 1990). Three main rock types, charnockite, granodiorite, and tonalite, make up this TTG unit. The tonalitic suite is mostly exposed in the north and is strongly mylonitized and retrogressed along the faulted boundary with the Pan-African orogenic belt, while granodiorites form distinct massifs within the dominantly charnockitic southern zone (Fig. 1). Exposures of supracrustal rocks (banded iron formations and sillimanite-bearing paragneisses) that represent remnants of greenstone belts form xenoliths in the TTG (e.g., Nsifa et al. 1993). Late- to post-tectonic granitoids and syenites intrude the TTG (e.g., Kornprobst et al. 1976, Nédélec 1990, Tchameni 1997, Tchameni et al. 2000, 2001, Shang et al. 2001a, b) and clearly postdate the major crustal-forming

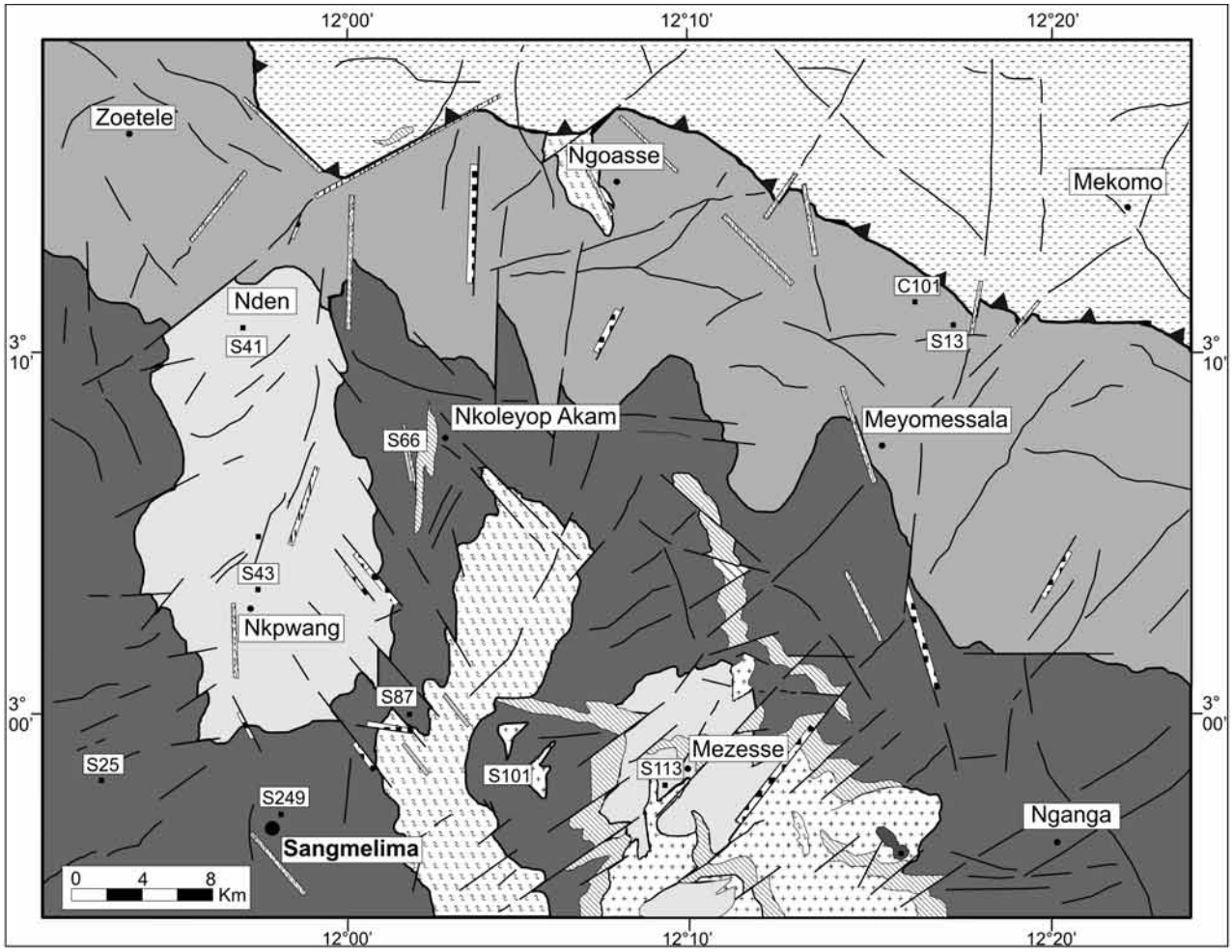

Pan-African belt
- Garnet-muscovite schists

Palaeoproterozoic
- Doleritic vein or dyke

Archaean
- Mylonitic band
- Granitic vein or dyke
- Monzogranite and syenogranite
- Garnet-hypersthene (TTG) migmatite gneiss
- Tonalitic suite (TTG)
- Granodiorite (TTG)
- Charnockitic suite (TTG)
- Meta-quartzites-iron trenches-Greenstone relics
- Faults and fractures
- Major thrust fault (Pan-African)

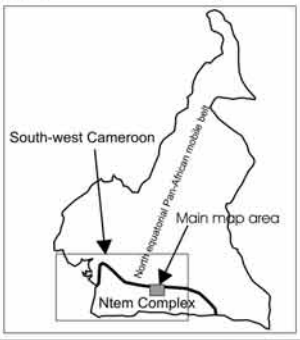

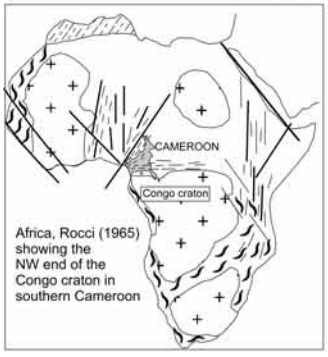

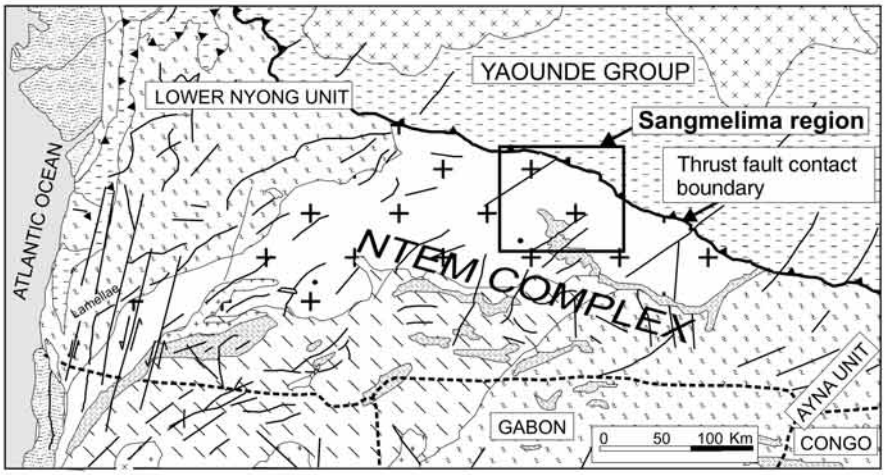

- Sedimentary cover
- Mbalmayo series
- Ntem unit (banded series, intrusive complex)

YAOUNDE GROUP
- Yaounde series

NTEM GROUP
- Ayna and Lower Nyong units

- Banded iron formations (greenstone belts relics)

South-west Cameroon (after Maurizot et al. 1986).

episode. Late Eburnean (*ca.* 2.1 Ga) doleritic dykes (e.g., Toteu et al. 1994, Vicat et al. 1996) represent the final magmatic activity in the Ntem complex.

Petro-structural studies suggest three major episodes of deformation in this geological domain. The first is characterized by vertical foliation and lineation, and isoclinal folds. These structural elements mark the diapiric emplacement of the TTGs (Shang 2001, Tchameni et al. 2001). The second major tectonothermal event is marked by the development of sinistral shear planes trending north-south to N45°E, with partial melting of the TTG and the greenstone belt country rock. Although the timing of this second event is not well constrained, Rb-Sr whole-rock data from Lasserre and Soba (1976) suggest that it occurred between 2400 Ma and 1800 Ma ago. Toteu et al. (1994) dated the peak of this metamorphism at about 2050 Ma using the U-Pb zircon method on metamorphic rocks from the Nyong series. Rb-Sr biotite ages of 1997 ± 19 Ma, 2064 ± 20 Ma, and 2299 ± 22 Ma (Shang et al. 2004) for the Sangmelima TTG tend to confirm this metamorphic episode for the Ntem complex. Although the third deformational indications pertain to the overthrusting Pan-African schistose formations, a multitude of C_3 structures (mylonitic and shear corridors) of Pan-African origin are observed in TTG rocks at the thrusting front.

The *charnockitic rocks* in the Sangmelima region form a suite from fine- to medium-grained norites, to medium- to coarse-grained felsic enderbites, charno-enderbites, and true charnockites often with diffuse contacts. Rocks of the *tonalitic suite* are medium- to coarse-grained leucocratic facies of trondhjemitic composition, mesocratic-melanocratic and medium-grained facies of dioritic composition, and mesocratic-leucocratic medium-grained facies of tonalitic composition. Dioritic facies with cumulate texture represent an early crystallized member of the tonalitic suite. *Granodiorites,* like the tonalites, are characterized by a conspicuous absence of hypersthene compared to members of the charnockitic suite. These rocks are dark grey and medium-to coarse-grained. Biotite is their major mafic mineral. Minor clinopyroxene and brown hornblende blebs are observed in association with green hornblende and oxides.

SiO_2 concentrations are consistent with the intermediate and acidic classifications of the Sangmelima TTG suite, and indicate fractional crystallization as the origin of the rock suites (e.g., Nédélec et al. 1990, Shang 2001). Although the Al index (A/CNK) indicates both metaluminous and peraluminous compositions, a predominantly metaluminous character is observed for members of the charnockitic suite, while a greater proportion of the tonalites and granodiorites show a peraluminous character (Shang 2001). The three TTG rock types are calc-alkaline, though the granodiorites reveal a slight potassic calc-alkaline tendency, while the tonalites and charnockites belong to the classic sodic calc-alkaline trend which is typical of Archaean TTG suites worldwide. Low average abundances in Pb (7.2 ppm), Th (3.7 ppm), and U (0.5 ppm) are found in rocks of the charnockitic suite. The average values of these elements in the tonalites are 11.1 ppm for Pb, 8.2 ppm for Th, and 0.6 ppm for U, while high average concentrations (Pb = 14.9 ppm, Th = 9.2 ppm, U = 0.8 ppm) are characteristic of the granodiorites. The negative Nb and Ta anomalies in these rocks are of great significance, as they are a distinctive characteristic of rocks derived from convergent plate margins. Trace element and REE characteristics distinguish two groups in the Sangmelima TTG (Shang et al. 2004). One group is marked by low REE abundance, positive Eu anomalies, and strong depletion in HREE; they probably represent rocks derived from felsic melts. The second group displays high REE abundance, negative Eu anomalies, and enrichment in HREE that may represent rocks from more fractionated melts. In general, tonalites and granodiorites that are more siliceous than the charnockites display higher LREE enrichment (Shang et al. 2004).

Table 1. Typologic % distribution of zircons from the Sangmelima TTG

% distribution	0–5%	5–10%	10–20%	20–40%	> 40%
Charnockitic suite	S_8, S_9, S_{10}, S_{15}, P_5, G_1, AB_2	P_3		S_{14}, S_{19}	
Tonalitic suite	S_{18}, S_{19}, S_{23}	S_{10}, S_{11}, S_{14}		S_{15}	P_3
Granodiorites	L_5, S_{12}		P_2	P_3, S_{15}	

Analytical techniques

Zircon microscopy and cathodoluminescence

It has long been recognized that zircons are variable in external morphology and that their internal zonation patterns are of petrogenetic and paragenetic significance (e.g., Poldervaart 1955, 1956, Poldervaart and Eckelmann 1955; Eckelmann and Kulp 1956). For this work, zircon grains were separated from 200–63 μm sieved rock fractions by standard separation techniques (milling, wet shaking table, magnetic and heavy liquid separation). The zircon grains were studied for morphological characterization using binocular and transmitted light microscopes to determine their typologic distribution, in accordance with Pupin (1980; Table 1). For dating purposes, and because of the complexity of natural zircon, the essential first step was to adequately document the internal structure of the zircon grains in order to better interpret the eventual geochronological data. Zircons were prepared as shown in Fig. 2. A cathodoluminescence (CL) imaging technique (e.g., Vavra 1990, 1994, Hanchar and Miller 1993, Hanchar and

←
Figure 1. Regional geological map of the northwestern part of the Congo craton (Ntem complex) and thrust contact with the North Equatorial Pan-African orogenic belt in South Cameroon. Main map shows the geology of the Sangmelima region and the distribution of the TTG suite.

Table 2. Evaporated zircon data including radiogenic $^{207}Pb/^{206}Pb$ ratios and corresponding age data for the Sangmelima TTGs

	Sample/grain No.		Zircon features	Evapo.temp. in °C	Th/U Zir.	Mean of $^{206}Pb/^{208}Pb$ ratios	Mean of $^{206}Pb/^{204}Pb$ ratios	No. of $^{207}Pb/^{206}Pb$ ratios	Mean of $^{207}Pb/^{206}Pb$ ratios	$^{207}Pb/^{206}Pb$ age (Ma)
Charnockitic	S66	-1	small, oval, dark-brown	1430	0.93	3.8	876	149	0.1977 ± 7	2808 ± 6
		-2	small, long, thin, brown	1460	1.00	3.5	904	190	0.2010 ± 10	2834 ± 8
		-3	small, oval, dark-brown	1430	0.91	2.1	1111	52	0.2027 ± 14	2849 ± 12
	S101	-1	medium, long, brown	1430	0.59	5.9	7463	525	0.2036 ± 7	2855 ± 6
		-3a	small, short, brown	1430	0.68	5.2	875	188	0.1961 ± 8	2794 ± 7
		-3b	small, short, brown	1460	0.69	5.2	847	150	0.1959 ± 5	2792 ± 4
		-4a	small, long, brown	1430	0.58	6.1	1027	104	0.1924 ± 13	2763 ± 12
		-4b	big, thick, brown	1460	0.61	5.6	4587	303	0.2036 ± 8	2856 ± 6
		-5	thick, long, brown	1430	0.56	6.1	5525	366	0.2046 ± 10	2863 ± 8
	S249	-1	thick, short, brown	1440	0.57	6.1	1745	490	0.2045 ± 9	2862 ± 7
		-2	thick, long, brown	1430	0.75	4.7	1600	302	0.2047 ± 7	2864 ± 7
suite		-3	medium, long, brown	1460	1.23	3.1	419	130	0.1916 ± 16	2756 ± 14
		-4a	very thick, long, brown	1430	0.76	4.6	7463	181	0.2047 ± 9	2864 ± 7
		-4b	very thick, long,brown	1460	0.67	5.1	8197	300	0.2068 ± 6	2881 ± 4
		-5	medium, short, brown	1430	0.78	4.7	196	134	0.1961 ± 13	2794 ± 11
	S87	-2	big, long, dark brown	1430	0.58	6.1	1157	180	0.2021 ± 14	2843 ± 11
		-3	small, short, dark-brown	1440	0.76	4.7	514	319	0.1976 ± 10	2807 ± 9
		-4	big, thick, brown	1430	0.70	5.0	1179	449	0.1998 ± 8	2825 ± 7
		-5	very big, thick, brown	1430	0.61	5.6	11364	453	0.2034 ± 5	2854 ± 4
	S25	-1	long, thick, brown	1420	0.67	5.3	615	190	0.2172 ± 13	2960 ± 10
		-2	long, very thick, brown	1400	0.84	4.3	525	190	0.2248 ± 13	3016 ± 10
		-3	short, thick, brown	1430	1.12	2.2	189	76	0.2073 ± 13	2884 ± 10
Granodiorites	S43	-1a	small, short, brown	1400	3.01	1.6	93	190	0.1843 ± 14	2692 ± 13
		-1b		1440	1.61	2.4	217	190	0.2136 ± 17	2933 ± 13
		-2a	short, thick, brown	1400	2.32	1.8	135	114	0.1930 ± 12	2768 ± 10
		-2b		1430	1.57	2.5	226	190	0.2119 ± 08	2920 ± 7
		-2c		1460	1.19	3.1	359	152	0.2245 ± 13	2999 ± 10
		-3a	small, thin, long, brown	1420	1.43	2.8	199	152	0.1976 ± 30	2806 ± 25
		-3b		1460	1.16	3.3	275	114	0.2204 ± 10	2983 ± 7
		-4a	very thin, long, brown	1400	0.87	4.3	372	152	0.2216 ± 06	2992 ± 4
		-4b		1430	0.86	3.9	300	38	0.2173 ± 15	2962 ± 11

Tab. 2, continued

Granodiorites	S43	-5a	thick, short, brown	1420	1.35	2.8	254	126	0.2007 ± 31	2831 ± 14
		-5b		1460	1.13	3.2	509	190	0.2217 ± 26	2933 ± 19
		-6a	thick, long, brown	1430	1.93	2.1	188	152	0.1975 ± 26	2806 ± 22
		-6b		1460	2.14	1.9	174	152	0.1917 ± 30	2757 ± 26
		-7a	short, thick, brown	1430	1.85	2.3	144	152	0.1823 ± 23	2674 ± 21
		-7b		1470	2.14	1.9	137	190	0.1837 ± 34	2686 ± 31
		-8a	very long, thick, brown	1400	1.45	2.7	227	144	0.2009 ± 25	2834 ± 20
		-8b		1420	1.46	2.6	244	152	0.2143 ± 17	2939 ± 13
		-8c		1460	1.21	3.1	358	190	0.2190 ± 11	2973 ± 8
		-9	very long, thick, brown	1430	2.39	2.3	604	149	0.1992 ± 33	2819 ± 28
		-10	very long, thick, brown	1470	1.10	3.1	408	210	0.2091 ± 23	2899 ± 18
	S113	-1	small, short, light-brown	1430		2.1	173	87	0.1840 ± 22	2689 ± 20
		-2a		1430	1.96	2.1	173	148	0.1860 ± 34	2707 ± 30
		-2b		1460		2.4	219	27	0.1904 ± 10	2745 ± 9
		-3a		1430		2.1	173	167	0.1863 ± 17	2709 ± 15
		-3b		1460		1.9	154	28	0.1844 ± 17	2693 ± 15
		-4a	small, short, light-brown	1430	2.20	1.9	150	143	0.1820 ± 26	2671 ± 25
		-4b	big, thick, short, brown	1460	27.02	0.13	162	1130	0.1998 ± 19	2824 ± 14
	S41	-4a	thick, clean-brown	1430	1.03	3.7	260	295	0.1904 ± 24	2745 ± 21
		-5	thick, clean, brown	1430	0.99	2.8	312	190	0.1951 ± 38	2786 ± 25
Tonalitic suite	S13	-4	small, short, light brown	1430	0.18	18.7	15625	65	0.1984 ± 10	2813 ± 8
		-5	small, long, brown	1430	0.70	4.9	10753	332	0.1998 ± 14	2825 ± 11
		-6	thick, short, brown	1430	0.63	5.4	12195	71	0.1845 ± 15	2694 ± 14
		-7	small, long, brown	1430	0.43	8.1	4425	107	0.1920 ± 08	2759 ± 7
		-9a	big, thick, brown	1400	0.49	7.0	9524	301	0.1975 ± 10	2806 ± 9
		-9b	big, long, brown	1430	0.49	7.0	9708	262	0.1972 ± 08	2803 ± 6
		-9c	long, thick, brown	1460	0.48	7.1	11111	37	0.1993 ± 06	2820 ± 5
	C101	-1	medium, clean, brown	1430	0.39	8.8	1224	81	0.1828 ± 19	2678 ± 17

a, b, c = different temperature steps of the same grain

Rudnick 1995, Vavra et al. 1996) on an electron microprobe (JEOL Superprobe, JXA-8900RL), working with an accelerating potential of 15kV and a 15–10 nA current beam, was employed.

Pb-Pb zircon evaporation technique

$^{207}Pb/^{206}Pb$ zircon ages were obtained from chemically untreated but abraded zircons (e.g., Krogh 1982) by the single zircon grain Pb evaporation procedure, the principles of which are described in Kober (1986, 1987), Kröner and Todt (1988), Cocherie et al. (1992), and Klötzli (1999). Measurement was done using a Finnigan MAT 262 mass spectrometer equipped with a MassCom ion counter. In our experiments, the temperatures of the evaporation filament were increased in 20 or 30 °C increments during repeated evaporation steps. The evaporated zircons were not those taken for CL analyses, but were representative of those investigated by CL. Only data of more than 30,000 counts per second for ^{206}Pb and with a high radiogenic Pb component ($^{206}Pb/^{204}Pb > 5000$) are usually considered for evaluation; however, in the present work, we also used data with $^{206}Pb/^{204}Pb < 5000$ due to the high common lead composition of most of the grains analyzed (Table 2). The radiogenic $^{207}Pb/^{206}Pb$ ratios were calculated according to the formula given in Cocherie et al. (1992). No correction was made for mass fractionation, which was significantly less than the uncertainty of the measured Pb isotope ratios. The common Pb corrected $^{207}Pb/^{206}Pb$ ratios normally define a Gaussian distribution, from which the mean of the $^{207}Pb/^{206}Pb$ ratios was derived. For error estimation, a 1σ error of the Gaussian distribution function was applied to all measured $^{207}Pb/^{206}Pb$ ratios (between 34 and 500 per grain). Our technique was tested on natural zircons from the Phalaborwa igneous complex, South Africa (Eriksson 1984, Verwoerd 1986), and zircon 91500 from Kuehl lake, Ontario, Canada (Wiedenbeck et al. 1995), which has been used as standard material in many laboratories (e.g., Kröner and Willner 1998, Wiedenbeck et al. 1995), the results of which are published in Chen et al. (2002).

U-Pb isotope analyses

U-Pb isotope and common Pb analyses were performed on zircons and K-feldspars, respectively. Zircons (i.e. one to three grains) were washed in 6N HCl then 7N HNO_3, spiked with a $^{205}Pb/^{235}U$ tracer solution, and dissolved in HF at 200°C for 6 days in a Parr bomb, as described by Parrish (1987). Separation and purification of U and Pb was carried out in Teflon columns with a 40-µl bed of AG1-X8 (100–200 mesh) and employing a HBr-HCl wash and elution procedure. K-feldspar was first washed in 2N HCl for a few minutes and leached in 6N HCl and then in 7N HNO_3. Residues were decomposed in hot 22N HF. Feldspar Pb was separated with the help of a funnel containing an 80 µl bed of AG1-X8 (100–200 mesh) anion exchange medium and employing a HBr-HCl wash and elution procedure, then in 40 µl columns for cleaning.

Pb was loaded with a mixture of Si gel and H_3PO_4 onto a single-Re filament and measured at ~ 1300 °C. U was loaded with 1N HNO_3 and measured in a double Re-configuration mode. The thermal fractionation of Pb standard NBS 981 was measured, and the isotopic ratios corrected for 0.11% fractionation per atomic mass unit. All measurements were performed with a Finnigan MAT 262 multicollector mass spectrometer operated in a static collection mode. Corrections for the remaining initial common Pb after the correction for tracer and blank were done using values from the Stacey and Kramers model (1975). Total procedural blanks for Pb and U were less than 10 pg. The U-Pb data were evaluated with the Pbdat program (Ludwig 1988). Data regression analysis was performed using the algorithm regression treatment according to Wendt (1986). Data was also treated without assumption for common Pb using Wendt's 3D model (1984). Plots were made by use of Isoplot/Ex program version 2.06 (Ludwig 1999).

Results

Zircon internal structure and morphology

CL images of selected zircons from Sangmelima TTG are presented in Fig. 3. The internal structure of these zircons suggests a complex crystallization-recrystallization history. In the simplest cases some distinctive zones are observed in most of the zircons from the three TTG rock types: a characteristic euhedral magmatic oscillatory zonation of variable CL intensities that represents growth bands of variable trace element and REE concentrations within zircon (e.g., Köppel and Sommerauer 1974, Hanchar and Miller 1993), although CL intensities in some cases have also been reported to be dependent on lattice defects (e.g., Pidgeon 1992, Geisler and Pidgeon 2001). Some of the zircons show irregularly shaped areas overprinting the zoning (e.g., S87-1, S43-6). There are also unzoned segments of rounded cores of inherited zircon, and irregularly shaped patches of unzoned or faintly zoned zircon that appear to have partially or wholly replaced zoned zircon. Bright areas of CL are in some cases seen to project through the body of the crystal as volumes of faintly zoned zircon, having either sharp or diffuse boundaries (e.g., S25-7) with the surrounding zoned zircon. More complex patterns observed in some of these structures probably represent melt resorption-dissolution features and recrystallized zircon that are often accompanied by Pb and U loss (e.g., van Breemen et al. 1987, Vavra 1990, Pidgeon 1992). Backscattered images also show highly fractured zircon (cracks and channels), evidence that the primary magmatic zircon has been affected by brittle deformation.

A careful morphological study and comparison with the classification by Pupin (1980) led us to determine zircon typologic distribution in the Sangmelima TTG (Table 1). The zircons are euhedral with characteristic prismatic and pyramidal crystal faces. The combination of these faces exhibit oval, somewhat discoidal, hexagonal,

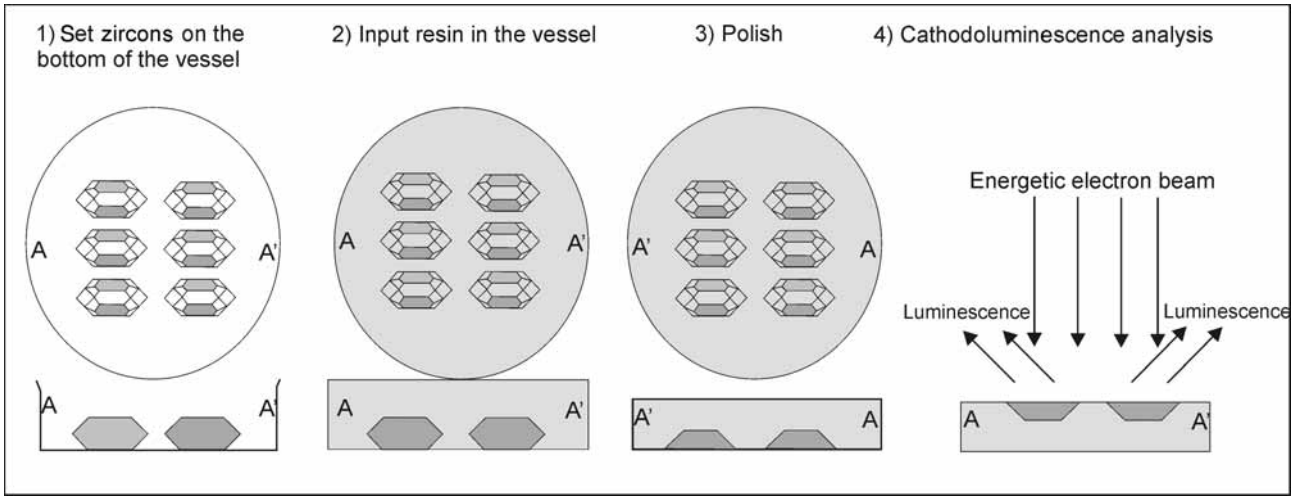

Figure 2. Procedure for fixing zircon grains for cathodoluminescence analysis.

and prismatic morphologies with long and thick or short and thick forms. The zircons are brown to reddish and/or dark brown, opaque and occasionally translucent, and sometimes contain inclusions. They range in size from ~ 65 μm to ~ 120 μm in width and up to 180 μm in length. Most of the investigated zircon crystals from the charnockitic suite, tonalites, and granodiorites show crystallographic characteristics of the S and P types, with very few AB_2, G_1, and L_5 subtypes (Table 1) as described by Pupin (1980). Geothermometric implications according to Pupin (1980) correspond to temperatures of between 600 ± 50 °C and 850 ± 50 °C with the main range between 700–800 °C.

$^{207}Pb/^{206}Pb$ evaporation data

Representative rock samples of the charnockitic suite from which separated zircons were analysed include a charnoenderbite (S66), a monzonorite (S101), a norite-monzonorite (S249), and enderbites (S87 and S25). Three zircons from S66 gave $^{207}Pb/^{206}Pb$ dates between 2808 ± 6 Ma and 2849 ± 12 Ma (Table 2). Four zircons from S101 yielded dates ranging from 2763 ± 12 Ma to 2863 ± 8 Ma. Grain 3 gave two similar dates for two temperature steps with a mean of 2793 ± 4 Ma while grains 1, 4b, and 5 yielded similar dates within the error limit, with a mean date of 2857 ± 4 Ma. Five zircons from sample S249 were analysed. Three of these (1, 2, and 4a) gave similar dates within uncertainty limits, the weighed mean of which is 2863 ± 4 Ma, while two different dates at different temperature steps of 2864 ± 7 Ma at 1430°C and 2881 ± 4 Ma at 1460 °C were obtained from grain 4. Grains 3 and 5 yielded two younger dates < 2800 Ma. Four zircons from sample S87 yielded dates ranging from 2807 ± 9 Ma to 2854 ± 4 Ma, being very similar to dates from sample S66. Grains 2 and 5 have identical dates within the uncertainty limit with a weighed mean of 2853 ± 4 Ma. The oldest date (2854 ± 4 Ma) is similar to those from sample S101. Three distinct dates were obtained from three different zircons from S25; 2884 ± 10 Ma for grain 3, 2960 ± 10 Ma for grain 1, and 3016 ± 10 Ma for grain 2 (Table 2).

The representative rock samples of the tonalitic suite from which zircons were separated for Pb-Pb chronometry are the tonalitic C101 and the trondhjemitic S13. One zircon from C101 yielded a $^{207}Pb/^{206}Pb$ date of 2678 ± 17 Ma. Five zircons from S13 yielded $^{207}Pb/^{206}Pb$ dates between 2694-2825 Ma (Table 2), with five of the analyses giving similar dates between 2803 and 2825 Ma. Grain 4 gave a date of 2813 ± 8 Ma while an older date of 2825 ± 11 Ma was obtained from grain 5. Three similar dates were obtained at three different temperature steps from grain 9; 2803 ± 6 Ma (9b), 2806 ± 9 Ma (9a), and 2820 ± 5 Ma (9c). Grains 5 and 9c yielded very similar dates while the same date within error limits was obtained from grain 4 and 9a. Grains 6 and 7 gave younger $^{207}Pb/^{206}Pb$ dates of 2694 ± 14 Ma and 2759 ± 7 Ma, respectively.

The granodiorite samples from which zircons were separated are S43, S113, and S41. Eight zircons from S43 yielded numerous dates (Table 2). A young date of 2692 ± 13 Ma from grain 1a is similar to two dates from grain 7 (2674 ± 21 Ma and 2686 ± 31 Ma), though these are much younger than the young dates obtained from other zircons. Four zircons from S113 gave variable but similar dates in most cases. Grain 1 yielded a date of 2689 ± 20 Ma. A similar date of 2693 ± 15 Ma was obtained for 3b, 2707 ± 30 Ma for 2a, and 2709 ± 15 Ma for 3a. Grain 4a, however, gave a young date of 2671 ± 25 Ma, while relatively older dates of 2745 ± 9 Ma and 2824 ± 14 Ma were obtained from grains 2b and 4b, respectively. Two zircons from S41 yielded two slightly different dates of 2745 ± 21 Ma and 2786 ± 25 Ma.

U-Pb data

U-Pb isotope dilution analyses for rocks of the charnockitic suite and granodiorites were attempted on zircons with magmatic habit. The results obtained for eight zircon fractions from sample S25 (monzonorite), and from three fractions from S43 (granodiorite), are presented in Table 3 and displayed graphically in Fig. 4. Data from both rock types plot below the concordia curve. The percentage degree of discordance calculated from a given $^{207}Pb/^{206}Pb$ date and the

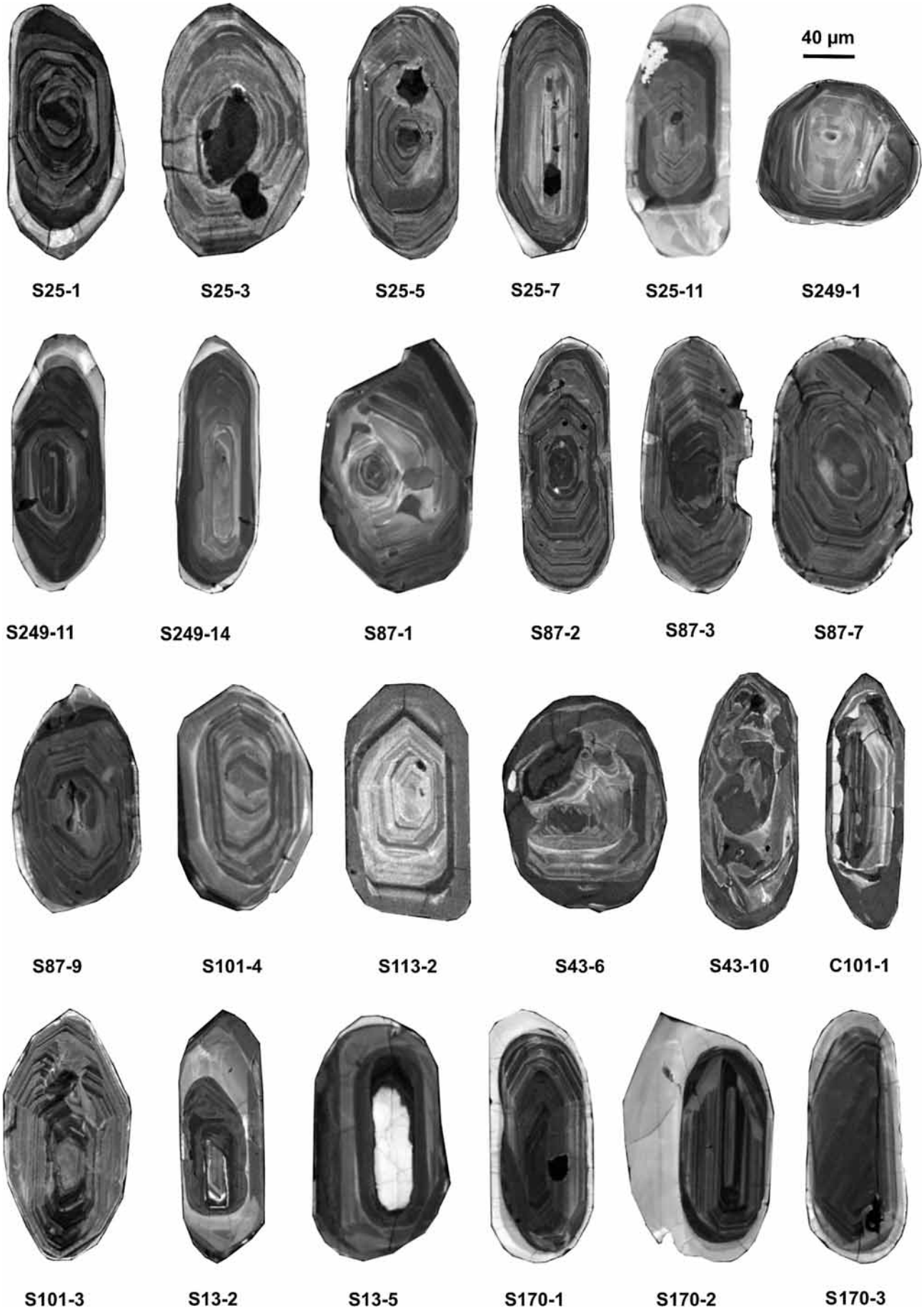
40 µm
S25-1
S25-3
S25-5
S25-7
S25-11
S249-1
S249-11
S249-14
S87-1
S87-2
S87-3
S87-7
S87-9
S101-4
S113-2
S43-6
S43-10
C101-1
S101-3
S13-2
S13-5
S170-1
S170-2
S170-3

lower intercept age are very similar: they range from 43.0% to 60.4% for zircon fractions from sample S25, and from 41.7% to 51.0% for those from sample S43 (Table 3). While the datum point for fraction 6 (S25) plots above the main regression trend as defined by the other five data points, data for fractions 2 and 8 plot below it (Fig. 4b). On the other hand, three data points from S43 describe a well defined linear arrangement. Discordias for the two data plots calculated for 2900 Ma Stacey and Kramers (1975) Pb portray lower Pan-African and upper Archaean intercept age of 492 ± 10 Ma and 2928 ± 17 Ma, respectively, for S25 with an MSWD of 25, and 602 ± 34 Ma and 3085 ± 26 Ma, respectively, for S43 with an MSWD of 0.35. For comparison, Pan-African (550 Ma) Stacey and Kramers (1975) Pb was also applied and similar results were obtained. In fact, data points for S25 yielded a lower Pan-African intercept age of 486 ± 9 Ma and an upper Archaean intercept age of 2929 ± 6 Ma, MSWD = 28, while data for S43 yielded a lower and upper intercept ages of 573 ± 32 Ma and 3076 ± 26 Ma, with MSWD = 0.002 (Table 4). The U-Pb data were also corrected with the measured average K-feldspar Pb [(^{206}Pb/^{204}Pb)i = 14.61 and (^{207}Pb/^{204}Pb)i = 15.3], calculated back to 2900 Ma using measured U concentrations (between 0.0026 and 0.076 ppm). The results yielded lower and upper intercept ages for S25 of 594 ± 25 Ma and 2945 ± 16 Ma, respectively, with MSWD = 23; and 606 ± 34 Ma and 3058 ± 26 Ma, with MSWD = 0.15 for S43 (Table 4). An independent control using the three dimensional U-Pb model of Wendt (1984), which allows the evaluation of Pb data for samples of unknown common Pb composition, gave lower and upper intercept ages of 477 ± 28 Ma and 2984 ± 24 Ma and a MSWD = 4.7 for S25, and 565 ± 41 Ma and 3094 ± 37 Ma, with MSWD = 0.01 for S43 (Table 4).

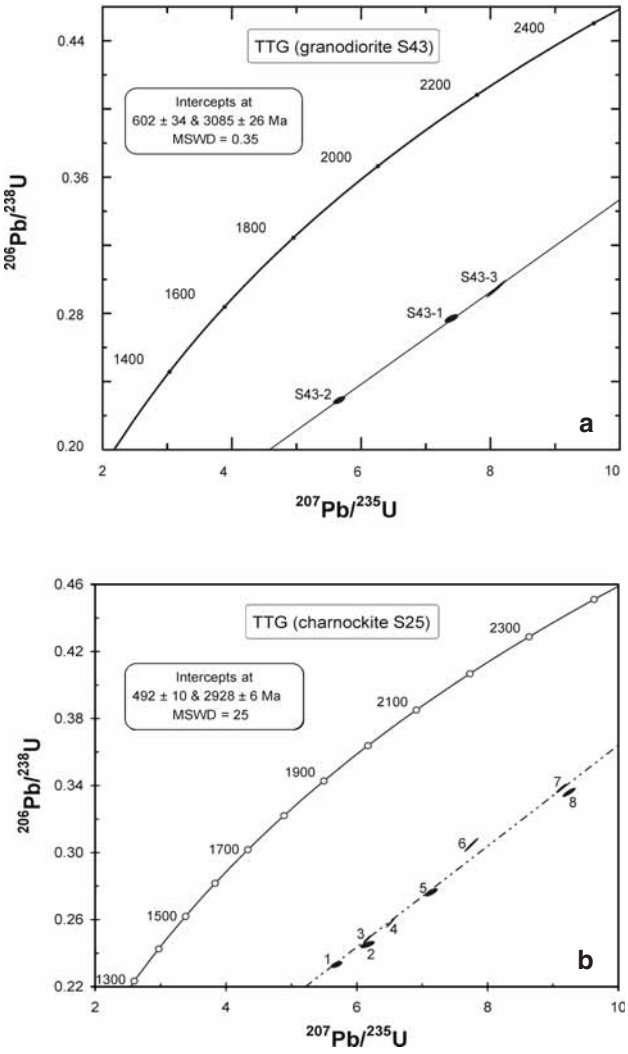

Figure 4. (a) U-Pb concordia diagram with three data points from abraded zircons (e.g., Krogh 1982) from granodiorites (S43) that define a lower intercept Pan-African age (602 ± 34 Ma), and an upper intercept Archaean age (3085 ± 26 Ma); (b) U-Pb concordia diagram with eight data points from abraded zircons of the charnockitic suite (S25), showing a lower intercept Pan-African age (492 ± 10 Ma) and an upper intercept Archaean age (2928 ± 6 Ma). Data corrected for Archaean Pb (see Table 4 for more data).

Th/U ratios and U-Pb budget

Th/U ratios (Tables 2 and 3) for Sangmelima zircons were calculated from Pb-Pb evaporation and U-Pb isotope dilution data using measured ^{206}Pb/^{208}Pb ratios and the apparent ^{207}Pb/^{206}Pb dates. Th/U ratios from charnockite zircon evaporation data mostly vary from 0.56 to 0.93, though three of the 22 analysed zircons yielded higher ratios of 1.00 to 1.23. Ratios between 0.18 and 0.70 were obtained for zircons from the tonalites. Granodiorite zircons on the other hand gave relatively high ratios of 0.86 to 3.01. Grain S113-4b (Table 2) evaporated at a high temperature of 1460 °C, however yielded a very high Th/U ratio of 27 thought to be due to a Th-rich inclusion (e.g., Hinton and Upton 1991). High Th-rich minerals commonly found as inclusions in zircon, and therefore possible sources of Th are thorite ($ThSiO_4$), thorianite [$(Th,U)O_2$], monazite [$(Ce,La,Ya,Th,U)PO_4$], xenotime [$(Y,REE,Th,U)PO_4$], and coffinite [$(U,Th)SiO_4$]. Th/U ratios determined from U-Pb isotope dilution analyses (Table 3) vary from 0.54 to 0.71 for fractions from charnockitic sample S25. Th/U ratios from granodiorite S43 range from 0.82 to 0.98 (Table 3). For comparison, whole-rock Th/U ratios vary from 0.5 to 9.6 for the charnockites, 0.5 to 9.2 for tonalites, and 0.4 to 16.1 for granodiorites, with average values of 5.0, 4.6, and 6.7, respectively (Shang et al. 2004).

The Pb and U concentrations of the zircons (Table 5) were determined from isotope dilution data for charnockitic rocks and granodiorites. Both rock types show particularly low ^{206}Pb/^{204}Pb ratios compared to tonalites (Table 2). Total Pb concentrations range from 142 ppm to 216 ppm for the charnockitic suite, with common Pb concentrations of

←
Figure 3. Cathodoluminescence micro-photographs of the characteristic zircon populations of the Sangmelima TTG suite; S25, S249, S87, S101 = charnockitic suite; S113, S43 = granodiorites; C101, S13, S170 = tonalitic suite. The zircons are 100 to 180 μm long and 63 to 100 μm wide.

Table 3. Zircon U-Pb analytical data of the Sangmelima region charnockitic sample and a granodiorite corrected for Archaean common Pb according to the two stage evolution model of Stacey and Kramers (1975).

Zircon description	Sample weight in mg*	$^{206}Pb/^{204}Pb$	U(ppm)	Pb(ppm)	Th/U	Atomic ratios				Apparent ages (Ma)			
						$^{208}Pb^*/^{206}Pb^*$	$^{206}Pb/^{238}U$	$^{207}Pb/^{235}U$	$^{207}Pb^*/^{206}Pb^*$	Degree of discordance in %	$^{206}Pb^*/^{238}U$	$^{207}Pb^*/^{235}U$	$^{207}Pb^*/^{206}Pb^*$
Charnockitic suite (S25)													
1 thick, long	0.048	142	429	209	0.65	0.19167	0.30495 ± 31	7.7665 ± 13	0.18472 ± 02	56.3	1716	2204	2696
2 thin, long	0.050	159	331	142	0.63	0.18413	0.27634 ± 17	7.1379 ± 68	0.18734 ± 11	49.9	1573	2129	2719
3 thick, short	0.065	210	434	216	0.71	0.20688	0.33607 ± 18	9.2470 ± 68	0.19956 ± 08	59.2	1869	2363	2823
4 small, oval	0.040	104	346	147	0.54	0.15751	0.24521 ± 14	6.1638 ± 81	0.18231 ± 18	44.5	1414	1999	2674
5 thick, oval	0.025	126	496	188	0.57	0.16599	0.23340 ± 13	5.6912 ± 64	0.17685 ± 15	43.0	1352	1930	2624
6 thick, short	0.064	122	447	190	0.54	0.15589	0.25797 ± 14	6.5154 ± 37	0.18317 ± 15	47.0	1410	2048	2682
7 thick, long	0.064	105	213	92.4	0.57	0.16718	0.24835 ± 18	6.1579 ± 45	0.17984 ± 18	45.6	1430	1999	2651
8 thin, short	0.044	197	492	244	0.58	0.16815	0.33824 ± 20	9.1300 ± 56	0.19576 ± 17	60.4	1879	2351	2791
Granodiorite (S43)													
1 short, thick	0.026	158	519	249	0.94	0.27602	0.29419 ± 30	8.0675 ± 83	0.19888 ± 02	51.0	1662	2239	2817
2 long, thin	0.060	131	462	177	0.82	0.23873	0.22904 ± 15	5.6603 ± 64	0.17924 ± 14	41.7	1330	1925	2646
3 thick, long	0.025	137	422	199	0.98	0.28594	0.27701 ± 17	7.3972 ± 75	0.19367 ± 13	49.2	1576	2161	2774

All errors quoted are 2σ absolute uncertainties and refer to the last digit
* radiogenic ; grain size varies from 80–180 µm
mg* error in weight is estimated to be up to 10%
% degree of discordance determined for the given $^{207}Pb/^{206}Pb$ age and the Pan-African lower intercept

34 ppm to 54 ppm, giving an average common Pb content of 26.2% (Table 5). U concentrations vary from 332 ppm to 496 ppm. Total Pb concentrations for granodiorites range from 177 ppm to 249 ppm. Common Pb concentrations vary from 48 ppm to 56 ppm, yielding an average common Pb content of 24.2%. U concentrations in granodiorites vary from 422 ppm to 519 ppm.

Discussion

Geochronolgy

Multiple $^{207}Pb/^{206}Pb$ evaporation dates were obtained from zircons from each of the Sangmelima TTG rock type. The histogram presented in Fig. 5 displays the frequency distribution of $^{207}Pb/^{206}Pb$ zircon age data, and includes 23 dates for the charnockitic suite, 8 for the tonalitic suite, and 29 for granodiorites. Given the internal structure of the zircons, (with their oscillatory magmatic zoning, relict cores, recrystallization overprints, and resorption-dissolution features), these Pb-Pb zircon evaporation data are interpreted to represent crystallization ages, mixing ages due to various degrees of inheritance, and data without geological meaning due to Pb loss.

We interpret dates > 2850 Ma and nearer to 2880 Ma for the charnockitic suite (Fig. 5) as a close approximation of their emplacement time. While the date of 2834 Ma could represent emplacement timing for granodiorites, we believe that the older date from tonalites (2825 Ma) is their probable crystallization age. The date of 2884 ± 10 Ma for grain S25-3 of the charnockitic suite is within the uncertainty limits nearly identical with the 2896 ± 7 Ma date reported by Toteu et al. (1994) on a population of zircons from charnockites from parts of the Ntem complex by the conventional U-Pb method, and near the date of 2912 ± 1 Ma obtained through the single grain evaporation method reported by Tchameni (1997) for zircons from charnockites of the Ebolowa region. In the latter region, data from a tonalitic zircon sample taken from the same outcrop as the charnockites yielded a $^{207}Pb/^{206}Pb$ date of 2833 Ma (Tchameni 1997). This date is similar within the uncertainty limit to the $^{207}Pb/^{206}Pb$ date (2825 ± 11 Ma) obtained from grain S13-5 (Table 2). These results tend to confirm post-charnockitic emplacement for the tonalites and granodiorites as interpreted from field relations. This chronology has already been suggested by Toteu et al. (1994), who proposed a mean crystallization age of 2850 Ma for So'o tonalites.

The very old $^{207}Pb/^{206}Pb$ evaporation dates from the charnockitic suite (2960 ± 10 Ma and 3016 ± 10 Ma), and similar dates in granodiorites (2899 ± 18 Ma to 2999 ± 10 Ma), are thought to reflect the presence of an inherited Pb component. These $^{207}Pb/^{206}Pb$ dates are very similar to the Nd model ages (2990–3040 Ma T_{DM} model age and 2889-3027 Ma T_{CHUR} model age) for these rocks (e.g., Shang 2001, Shang et al. 2004), and therefore might indicate the formation age of the Ntem Archaean proto-crust.

Younger $^{207}Pb/^{206}Pb$ dates in the three TTG rock types are spurious, without geological meaning, and could be signatures of varying degrees of Pb loss during the geological history of the rocks (e.g., Corfu and Ayres 1984, Harrison et al. 1987, Kröner et al. 1994, Hanchar and Rudnick 1995, Whitehouse et al. 1999). Relatively well constrained young dates from 2854 to 2864 Ma (7 dates), 2825–2834 Ma (3 dates), 2792-2808 Ma (5 dates), and 2756–2763 Ma (2 dates) are found in the charnockitic samples. Data from granodiorites and tonalites also show such young dates that could similarly be signatures for varying degrees of Pb loss during a subsequent metamorphic event.

Zircon (U)-Pb systematics and regional implications

It is well known that zircons can loose their radiogenic Pb by diffusion. This process is accelerated by heat, fluid, radiation damage, uplift, and surface weathering (e.g., Wetherill 1956, Wasserburg 1963). Diffusional Pb loss can be linked to chemical alteration (e.g., Corfu and Ayres 1984) to which certain zircon compositions are especially susceptible (e.g., Corfu 2000). The Sangmelima zircons show clear evidence of Pb loss. Recrystallization and dissolution features, such as relict oscillatory zoning and faint and discontinuous zoning, are seen in the CL images (Fig. 3, grains S43-6, S43-10). Fractured zircons with cracks and channels (e.g., S25-1 and S25-3) demonstrate that the primary magmatic zircon has also been affected by brittle deformation. Zircons obtained from shear zones often show Pb loss caused by the higher fluid activities in those zones (e.g, Kröner et al. 1994; Nasdala et al. 1995; Mezger and Krogstad 1997). Zircons from the charnockites and granodiorites are further characterized by strongly discordant $^{207}Pb/^{235}U$ and $^{206}Pb/^{238}U$ ages (Figs 4a and 4b). Discordant U-Pb ages are generally attributed to Pb loss, the mixing of two or more zircon components of different ages, or some yet unknown process (e.g., Stern et al. 1966, Gebauer and Grünenfelder 1976, Black 1987). The existence of zircon domains with different ages within individual grains is well demonstrated by in situ analyses (e.g., Gebauer 1996, Vavra et al. 1996, 1999, Whitehouse et al. 1999). U-Pb data that define discordia can also be interpreted as a mixing array between the domains of older core material and younger overgrowths (e.g., Schmitz and Bowring 2000). However, CL evidence of structures that probably represent melt resorption-dissolution features and recrystallized zircon (e.g., Pidgeon 1992), strongly favors the Pb loss hypothesis for the Sangmelima zircons.

Table 4. Sangmelima TTG U-Pb concordia zircon age data (errors 2σ)

Corrected for Archaean (2900 Ma) Stacey and Kramers (1975) common Pb

S25 UI = 2928 ± 17 Ma	LI = 492 ± 10 Ma MSWD = 25
S43 UI = 3085 ± 26 Ma	LI = 602 ± 34 Ma MSWD = 0.35

Corrected for Pan-African (550 Ma) Stacey and Kramers (1975) common Pb

S25 UI = 2929 ± 6 Ma	LI = 486 ± 9 Ma MSWD = 28
S43 UI = 3076 ± 26 Ma	LI = 573 ± 32 Ma MSWD = 0.002

Corrected for K-feldspar common Pb (average $^{206}Pb/^{204}Pb$ of 14.61 and $^{207}Pb/^{204}Pb$ of 15.31 at 2900 Ma)

S25 UI = 2945 ± 16 Ma	LI = 594 ± 25 Ma MSWD = 23
S43 UI = 3058 ± 26 Ma	LI = 606 ± 34 Ma MSWD = 0.15

Uncorrected for common Pb, Tera-Wasserburg according to Wendt (1984)

S25 UI = 2935 ± 17 Ma	LI = 447 ± 28 Ma MSWD = 4.7
S43 UI = 3094 ± 37 Ma	LI = 565 ± 41 Ma MSWD = 0.01

UI = upper intercept
LI = lower intercept

Table 5. U and Pb concentrations in zircon fractions from Sangmelima TTG

Sample	U (ppm)	Pb_{total} (ppm)	Pb_{rad} (ppm)	Pb_{com} (ppm)	Pb_{com} in %
Charnockite					
S25-1	429	209	155	54	26
S25-2	332	142	108	34	24
S25-3	434	216	176	40	19
S25-4	346	147	98	49	33
S25-5	496	188	134	54	29
S25-6	447	190	133	57	30
S25-7	213	92	61	31	34
S25-8	492	244	196	49	20
Mean	398.6	178.5	133	46	26.9
Granodiorite					
S43-1	462	177	129	48	27
S43-4	422	199	149	50	25
S43old	519	249	193	56	22
Mean	467.6	208.3	157	51.3	24.6

Pb loss solely by radiation damage is not very likely for the Sangmelima zircons given their relatively low U concentrations (Table 3). Pb loss due to recent uplift and weathering can also be ruled out because the young $^{207}Pb/^{206}Pb$ evaporation dates can only be explained by non-recent Pb loss. Such a scenario is confirmed by the U-Pb discordia diagram. It seems most likely that Pb loss in zircons from the Sangmelima region occurred during a regional tectono-metamorphic event. A metamorphic overprint can enhance the rate of material exchange between

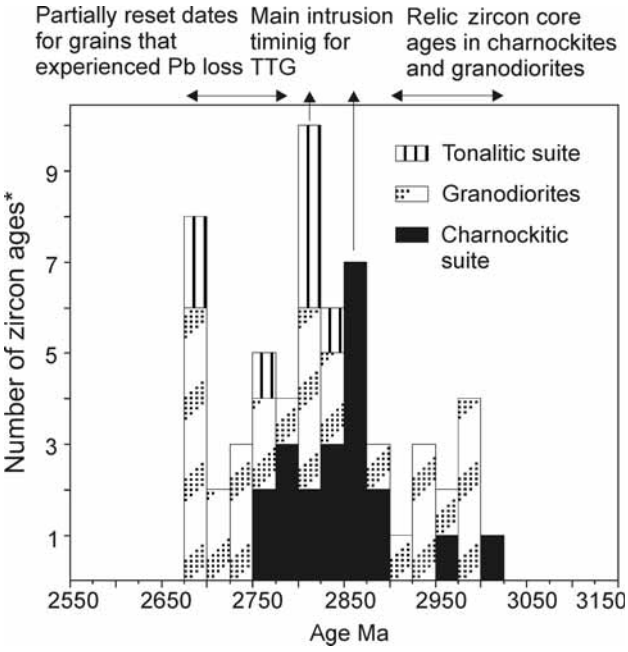

Figure 5. Histogram showing the distribution of zircon $^{207}Pb/^{206}Pb$ age data in the Sangmelima TTG suite.
* age of either single grains or different temperature steps of one grain as shown in Table 2.

zircon and a fluid phase. Although the timing of Pb loss in the Sangmelima TTG could be largely attributed to tectonothermal effects inflicted by the Eburnean and Pan-African orogenies on Archaean rock formations of the Congo craton as a whole, the conventional U-Pb zircon lower intercept ages found for the charnockite and the granodiorite samples (Fig. 4a and 4b and Table 4) indicate the Pan-African orogeny as the principal event responsible for Pb loss. These data indicate some thermodynamic influence from the overthrusting North Equatorial Pan-African orogenic belt (Nzenti et al. 1988; Nédélec et al. 1990; Tchameni 1997; Shang 2001) on the Ntem complex (Congo craton). In fact, similar age data have been reported by Toteu et al. (1994) on garnet amphibolites of the Ntem complex. Their investigations, also based on U-Pb zircon dating, found a lower discordia intercept age of 626 ± 26 Ma, thereby clearly showing the influence of the Pan-African orogeny on the Ntem complex.

While lower Pan-African discordia intercept ages could suggest the timing of Pb loss in our samples (Fig. 4), upper intercept Archaean ages could be indicative of the crystallization period. The remarkable similarity between the conventional Archaean U-Pb upper intercept zircon age for the Sangmelima TTG (2926 ± 6 Ma) from the charnockitic sample, the 3085 ± 26 Ma age from the granodiorite (Fig. 4), and the oldest $^{207}Pb/^{206}Pb$ evaporation dates from the same samples (Table 2, Fig. 5), as well as Nd model ages (2990–3040 Ma T_{DM} age and 2889–3027 Ma T_{CHUR} age, Shang et al. 2004), tend to indicate some inheritance from the protolith to the Sangmelima TTG rather than their true crystallization timing.

Common lead in Sangmelima zircons

It is worth noting that all zircon Pb evaporation analyses are characterized by particularly low $^{206}Pb/^{204}Pb$ ratios (Table 2) that vary from 189 to 11364 (mean = 2613) for rocks of the charnockitic suite, 1224 to 15625 (mean 9321) for the tonalites, and 93 to 1621 (mean 308) for the granodiorites. In theory such low ratios can be produced either by very low time integrated U concentration or by a high common Pb component. Based on the measured U concentrations of the analysed samples (213–519 ppm, Table 5), the low $^{206}Pb/^{204}Pb$ ratios must be explained by a high amount of common Pb. This unusually high proportion (19–34%) of common Pb in zircons of Archean age (Table 5), far above the usual zircon common Pb content of < 5% (e.g., Chen et al. 2002), points to common Pb intake. There are several possible explanations for the high common Pb concentrations in the Sangmelima TTG zircons: (1) the Congo craton could have been infiltrated by common Pb through plume activity, given the proximity of active volcanoes (notably Ngoma and the Cameroon line); (2) radiogenic Pb could have been preferentially leached from these zircons; (3) the present concentration could be a primary feature of the zircons. In fact, Pb evaporation data even at the highest temperature steps yield low $^{206}Pb/^{204}Pb$ ratios, suggesting that common lead is very well retained in the zircon's crystal lattice, a characteristic that would be related to intake during primary crystallization. However, the moderate whole rock average concentration of lead (7.3 ppm for the charnockitic suite, 11.1 ppm for the tonalitic suite, and 14.9 ppm for granodiorites; e.g., Shang et al. 2004), and the incompatibility of common lead in the zircon lattice makes a secondary lead intake in Sangmelima zircons more likely. In addition to the already demonstrated evidence of radiogenic Pb loss (Fig. 4), the high percentage of common Pb further distinguishes the zircons from the Sangmelima region as open systems.

Zircon Th/U ratios and petrologic implications

Zircon Th/U ratios determined from U-Pb isotope dilution analyses (Table 3) vary from 0.54 to 0.71 for fractions from charnockitic sample S25, and are similar to values from Pb evaporation data, while the values from granodiorite sample S43 range from 0.82 to 0.98 and are identical with lower values from the Pb evaporation data for the same rock type. Whole-rock Th/U ratios range from 0.5–9.6 for the charnockitic suite, 0.5–9.2 for members of the tonalitic suite, and 0.4–16.1 for granodiorites with average values of 5.0, 4.6, and 6.7, respectively (Shang et al. 2004). These Th/U ratios appear to show a correlation with zircon Th/U data (Table 2). In fact, low zircon Th/U ratios in charnockitic and tonalitic suites correspond to low Th/U whole-rock ratios, while high Th/U zircon ratios in granodiorites also reflect the high Th/U whole-rock ratios. This aspect suggests a systematic partitioning mechanism of Th and U in zircons and the whole rocks (e.g., Hoskin and Ireland 2000) of the Sangmelima TTG.

Considering all zircon data obtained in this study, Th/U ratios are generally moderate to high (0.18–3.01, Tables 2 and 3), and, in agreement with zircon internal structure, they are characteristic of magmatic zircons (e.g., Whitehouse et al. 1999). This is in contradiction to the lower ratios (~0.03) of metamorphic zircon (e.g., Kröner et al. 1994, Klötzli-Chowanetz et al. 1997, Klötzli 1999, Whitehouse et al. 1999), often attributed to the effect of the contemporaneous crystallization of monazite during metamorphism (e.g., Klötzli 1999).

The distribution coefficient of U in zircon is assumed to be 4–10 times higher than for Th (e.g., Mahood and Hildreth 1983). Given a whole rock Th/U ratio on the order of 4–7 for the Sangmelima TTGs (see below), Th/U ratios for magmatic zircon between 0.4 and 1 should be obtained. During magmatic differentiation toward highly evolved granitoids, Th/U ratios can strongly decrease (e.g., Klötzli 1999, Siebel et al. 2003). However, some charnockitic and most granodioritic fractions in the Sangmelima region show zircon Th/U ratios > 1. This suggests that Th could have been preferentially incorporated into the zircon lattice over U. The high Th/U ratios in Sangmelima TTG zircons could be justified by considering amphibolite or eclogite melting conditions for the source rock (e.g., Peacock et al. 1994; Sigmarsson et al. 1998). In fact, the experimental results of Peacock et al. (1994) suggest that the slow subduction of a young oceanic plate, partially melting under amphibolite or eclogite conditions, would yield adakitic melts of similar chemical compositions to TTGs and leave a solid residue principally composed of garnet and clinopyroxene. Since garnet's U partition coefficients are greater than for Th ($D_U > D_{Th;}$ e.g., Beatie 1993, LaTourette et al. 1993; Klötzli 1999), Th would be enriched relative to U in these partial melts, leading to high Th/U ratios. This aspect is equally portrayed in the whole-rock Th/U ratios for the Sangmelima TTG, with average values of 5.0, 4.6, and 6.7 for the charnockitic suite, tonalitic suite, and granodiorites, respectively. These are higher than the bulk earth estimates of 3.9 (Galer and O'Nions 1985) or 4.2 (Allègre et al. 1986), and a bulk continental crust value of 4.0 (Rudnick and Fountain 1995).

Conclusion

Obtaining reliable U-Pb and $^{207}Pb/^{206}Pb$ evaporation zircon ages on TTGs from the Sangmelima region has proven difficult due to complexities associated with the combined effects of Pb loss, inherited Pb components, and uptake of common Pb. A magmatic origin for the zircons is ascertained from the oscillatory zonation shown by CL imagery. Recrystallization signatures and brittle structures in some of the zircons suggest strong secondary effects in Sangmelima TTGs, and raise concerns that the U-Th systematics, like those of Pb-Pb, were disturbed, indicating a complex magmatic and post-magmatic history for the Sangmelima region.

Notwithstanding these difficulties, the U-Th-Pb system can still provide appropriate benchmarks for the petrogeneses of these rocks. The preservation of inherited zircons suggests that the rocks were derived from a > 2900 to 3200 Ma proto-crust. TTG magmatism in the Sangmelima region operated during the Mesoarchaean, between 2800 and 2900 Ma. Moreover, the following emplacement order was obtained from the $^{207}Pb/^{206}Pb$ isotope distribution pattern: charnockitic suite Õ granodiorites Õ tonalites.

Chemical and geochronological data show that the Sangmelima TTGs were probably derived from the partial melting of a subducting or thickening basaltic proto-crust of mantle origin. High Th/U ratios in the zircons and in the whole rocks point to the role played by residual garnet in the genesis of the Sangmelima TTG, as garnet's U partition coefficient is larger that that of Th under eclogite facies conditions.

The U-Pb lower discordia intercept ages suggest that post-emplacement thermo-tectonic events affecting the TTG rocks of the Sangmelima region were related to the Pan-African orogeny. This event caused significant reduction in the zircon radiogenic Pb budget, with consequent partial zircon age resetting. The uptake of common Pb could have been associated with this event, although the possibility that the high common Pb concentrations might be a primary feature of the zircons has not been completely ruled out.

Acknowledgements: The authors would like to thank the anonymous reviewers whose constructive and thorough criticisms led to the significant improvement of the manuscript. The first author (CKS) is highly indebted to the Department of Earth Sciences, Uni-Tübingen, St. Paulus Parish, Tübingen and the Kreim Family, Tuebingen, for hospitality, not forgetting the German Academic Exchange Service (DAAD) for initial support in this research project. Much gratitude goes to Matthias Westphal and Gregor Markl for use of microprobe facilities. CKS is also thankful to field colleagues from the University of Yaounde, Cameroon.

References

Allègre C. J., Dupré B., Lewin E. (1986): Thorium/uranium ratio of the Earth. Chem. Geol. 56, 219–227.

Beatie P. (1993): Uranium-thorium disequilibria and partitioning on melting garnet peridotite. Nature 362, 63–65.

Bessoles B., Trompette R. (1980): Géologie de l'Afrique: La Chaîne Pan-Africaine, „Zone mobile d'Afrique Centrale (partie Sud) et zone Soudanaise". Mémoire BRGM N° 92.

Black L. P. (1987): Recent Pb loss in zircon: a natural or laboratory induced phenomenon? Chem. Geol. 65, 25–33.

van Breemen O., Handerson J. B., Loveridge W. D., Thompson P. H. (1987): U-Pb zircon and monazite geochronology and zircon morphology of granulite and granite from the Thelon tectonic zone, Healey Lake map areas, N. W. T. In: Current Research Part A. Geol. Surv. Can. 87-1A, 783–801.

Cahen L., Delhal H., Lavreau J. (1976): The Archaean of Equatorial Africa: a review. In: Windley B. F. (ed.) The Early History of the Earth. Wiley, New York, 486–498.

Chen F., Siebel W., Satir M. (2002): Zircon U-Pb and Pb isotope fractionation during stepwise HF-acid leaching and geochronological implications. Chem. Geol. 191, 155–164.

Clifford T. N., Class I. G. (1970): African magmatism and tectonics. Olivier and Boyd. Edinburgh.

Cocherie A., Guerrot C., Rossi P. (1992): Single-zircon dating by step-wise Pb evaporation: Comparison with other geochronological techniques applied to the Hercynian granites of Corsica, France. Chem. Geol. 101, 131–141.

Corfu F. (2000): Extraction of Pb with artificially too-old ages during stepwise dissolution experiments on Archaean zircon. Lithos 53, 279–291.

Corfu F., Ayres L. D. (1984): U-Pb ages and genetic significance of heterogeneous zircon populations in rocks from the Favourable Lake area, northwestern Ontario. Contrib. Mineral. Petrol. 88, 86–101.

Delhal J., Ledent L. (1975): Donnée géochronologiques sur le complexe calcomagnésien du Sud Cameroon. Musée Royal d'Afrique Central (Belgium). Rap. Annu., 71–75.

Eckelmann F. D., Kulp J. L. (1956): The sedimentary origin and stratigraphic equivalence of the so-called Cranberry and Hendersen granites in western North Carolina. Am. J. Sci. 254, 288–315.

Eriksson S. C. (1984): Age of the Carbonatite and phoscorite magmatism of the Phalaborwa Complex (South Africa). Isot. Geosci. 2, 291–299.

Galer S. J. G., O'Nions R. K. (1985): Residence time of thorium, uranium and lead in the mantle with implications for mantle convection. Nature 316, 778–782.

Gebauer D. (1996): A P-T-t path for an (ultra?-)high pressure ultramafic/mafic rock association and its felsic country rock based on SHRIMP dating of magmatic and metamorphic zircon domains. Example: Alpe Arami, Central Swiss Alps. Earth Processes: Reading the Isotopic Code Geophys. Monogr. 95, 305–329.

Gebauer D., Grünenfelder M. (1976): U-Pb zircon and Rb-Sr whole rock dating of low-grade metasediments, example: Montagne Noir (southern France). Contrib. Mineral. Petrol. 59, 13–32.

Geisler T., Pidgeon R. T. (2001): Significance of radiation damage on the integral SEM cathodoluminescence intensity of zircon: an experimental annealing study. Neues Jahrb. Mineral.-Mon.hefte 10, 433–445.

Goodwin A. M. (1991): Precambrian Geology – The Dynamic evolution of the continental crust. Academic Press, New York.

Hanchar J. M., Miller C. F. (1993): Zircon zonation patterns as revealed by cathodoluminescence and backscattered electron images: Implications for interpretation of complex crustal histories. Chem. Geol. 110, 1–13.

Hanchar J. M., Rudnick R. L. (1995): Revealing hidden structures: The application of cathodoluminescence and back-scattered electron imaging to dating zircons from lower crustal xenoliths. Lithos 36, 289–303.

Harrison T. M., Aleinikoff J. N., Compston W. (1987): Observations and control of the occurrence of inherited zircon on concord-type granitoids, New Hampshire. Geochim. Cosmochim. Acta 51, 2549–2558.

Hinton R. W., Upton G. J. (1991): The chemistry of zircon: variations within and between large crystals from syenite and alkali xenoliths. Geochim. Cosmochim. Acta 55, 3287–3302.

Hoskin P. W. O., Ireland T. R. (2000): Rare earth element chemistry of zircon and its use as a provenance indicator. Geology 28, 627–630.

Klötzli U. S. (1999): Single zircon evaporation thermal ionisation mass spectrometry: Method and procedures. Analyst 122, 1239–1248.

Klötzli-Chowanetz E., Klötzli U. S., Koller F. (1997): Lower Ordovician migmatisation in the Ötztal crystalline basement/Austria: linking U-Pb and Pb-Pb dating with zircon morphology. Schweiz. Mineral. Petrogr. Mitt. 77, 315–324.

Kober B. (1986): Whole grain evaporation for $^{207}Pb/^{206}Pb$-age-investigations on single zircons using a double-filament thermal ion source. Contrib. Mineral. Petrol. 93, 482–490.

Kober B. (1987): Single zircon evaporation combined with Pb^{+} emitter bedding for $^{207}Pb/^{206}Pb$-age investigations using thermal ion mass spectrometry, and implications in zirconology. Contrib. Mineral. Petrol. 96, 63–71.

Köppel V., Sommerauer J. (1974): Trace elements and the behaviour of U-Pb system in inherited and newly formed zircons. Contrib. Mineral. Petrol. 43, 71–82.

Kornprobst J., Lasserre M., Rollet M., Soba D. (1976): Existence au Cameroun d'un magmatisme alcalin Pan-Africain ou plus ancient: la syénite néphélinique de Nkonglong. Comparaison avec les roches alcalines connues dans la męme région. Bull. Soc. Géol. Fr. 18, 1295–1305.

Krogh T. E. (1982): Improved accuracy of U-Pb zircon ages by the creation of more concordant systems using an air abrasion technique. Geochim. Cosmochim. Acta 46, 673–649.

Kröner A., Jaeckel P., Williams, I. S. (1994): Pb-loss patterns in zircons from a high grade metamorphic terrain as revealed by different dating methods: U-Pb and Pb-Pb ages of igneous and metamorphic zircons from Northern Sri Lanka. Precam. Res. 66, 151–181.

Kröner A., Todt W. (1988): Single zircon dating constraining the maximum age of the Barberton greenstone belt, southern Africa. J. Geophys. Res. 93, 15329–15337.

Kröner A., Willner A. P. (1998): Time of formation and peak of Variscan HP-HT metamorphism of quartz-feldspar rocks in the central Erzgebirge, Saxony, Germany. Contrib. Mineral. Petrol. 132, 1–20.

Lasserre M., Soba D. (1976): Age Libérien des granodiorites et des gneiss à pyroxènes du Cameroun Méridional. Bull. BRGM 2, 17–32.

LaTourette T. K., Kennedy A. K., Wasserburg G. J. (1993): Thorium-uranium fractionation by garnet: evidence for a deep source and rapid rise of oceanic basalts. Science 261, 739–931.

Ludwig K. R. (1988): Pbdat for MS-DOS – a computer program for IBM-PC compatibles for processing raw Pb-U-Th isotope data. Open-file Report 88–542, US Geol. Surv.

Ludwig K. R. (1999): Isoplot/Ex, version 2.06: a geochronological tool-kit for Microsoft Excel. Berkeley Geochronology Center Spec. Pub. 1a, 1–49.

Mahood G., Hildreth W. (1983): Large partition coefficients for trace elements in high-silica rhyolites. Geochim. Cosmochim. Acta. 47, 11–30.

Maurizot P., Abessolo A., Feybesse J. L., Johan Lecomte P. (1986): Etude de prospection minière du Sud-Ouest Cameroun. Synthèse des travaux de 1978 à 1985. Rapp. BRGM. 85, CMR 066.

Mezger K., Krogstad E. J. (1997): Interpretation of discordant U-Pb zircon ages: An evaluation. J. Metamorph. Geol. 15, 127–140.

Nasdala L., Irmer G., Wolf D. (1995): The degree of metamictization in zircon, a Raman spectroscopic study. Eur. J. Mineral. 7, 471–478.

Nédélec A. (1990): Late calcalkaline Plutonism in the Archaean Ntem unit: the Sangmelima granodioritic suite (South Cameroon). Et. Réc. Géol. Afrique, 25–28.

Nédélec A., Nsifa E. N., Martin H. (1990): Major and trace element geochemistry of the Archaean Ntem plutonic complex (South Cameroon): petrogenesis and crustal evolution. Precambrian Res. 47, 35–50.

Nsifa E. N., Tchameni R., Belinga S. M. E. (1993): De l'existence de formation catarchéennes dans le complex cratonique du Ntem (Sud-Cameroun). Project N° 273, Archaean cratonic rocks of Africa. Abst. Vol. p. 23.

Nzenti J. P., Barbey P., Macaudière J., Soba D. (1988): Origin and evolution of the late Precambrian high-grade Yaounde gneisses (Cameroon). Precambrian Res. 38, 91–109.

Parrish R. R. (1987): An improved micro-capsule for zircon dissolution in U-Pb geochronology. Chem. Geol. 66, 99–102.

Peacock S. M., Rushmer T., Thompson A. B. (1994): Partial melting of subducted oceanic crust. Earth Planet. Sci. Lett. 121, 227–244.

Pidgeon R. T. (1992): Recrsytallisation of oscillatory zoned zircon: some geochronological and petrological implications. Contrib. Mineral. Petrol. 110, 463–472.

Poldervaart A. (1955): Zircon in rocks, 1. Sedimentary rocks. Am. J. Sci. 253, 433–461.

Poldervaart A. (1956): Zircons in rocks, 2. Igneous rocks. Am. J. Sci. 254, 521–554.

Poldervaart A., Eckelmann F. D. (1955): Growth phenomena in zircon of autochthonous granites. Geol. Soc. Am. Bull. 66, 947–948.

Pupin J. P. (1980): Zircon and granite Petrology. Contrib. Mineral. Petrol. 73, 207–220.

Rudnick R. L., Fountain D. M. (1995): Nature and composition of the continental crust, a lower crustal perspective: Rev. Geophys. 33, 267–309.

Schmitz M. D., and Bowring S. A. (2000): The significance of U-Pb zircon dates in lower crustal xenoliths from the southwestern margin of the Kaapvaal craton, South Africa. Chem. Geol. 172, 59–76.

Shang C. K. (2001): Geology, Geochemistry and Geochronolgy of Archaean rocks from the Sangmelima Region, Ntem complex, NW Congo Craton, South Cameroon. Ph.D Thesis, University of Tübingen, Germany.

Shang C. K., Taubald H., Satir M., Siebel W., Nsifa E. N., Vennemann T., Njilah I. K., Ghogomu R. (2001a): Evidence for a non-cogenetic relationship between monzogranites and TTG suite: Abst. Vol. EUG XI, Strasbourg, France.

Shang C. K., Satir M., Siebel W., Taubald H., Nsifa E. N., Westphal M., Reitter E. (2001b): Genesis of K-rich granitoids in the Sangmelima

region, Ntem complex (Congo craton), Cameroon. Terra Nostra 5, 60–63.

Shang C. K., Satir M., Siebel W., Nsifa E. N., Taubald H., Liegeois J. P., Tchoua F. M. (2004): Major and trace element geochemistry, Rb-Sr and Sm-Nd systematics of TTG magmatism in the Congo craton: case of the Sangmelima region, Ntem complex, southern Cameroon. J. Afr. Earth. Sci. 40, 61–79.

Siebel W., Chen F., Satir M. (2003): Late-Variscan magmatism revisited: new implications from Pb-evaporation zircon ages on the emplacement of redwitzites and granites in NE Bavaria. Int. J. Earth. Sci. 92, 36–53.

Sigmarsson O., Martin H., Knowles J. (1998): Melting of a subducting oceanic crust from U-Th disequilibra in austral Andean lavas. Nature 394, 566–569.

Stacey J. S., Kramers J. D. (1975): Approximation of terrestrial lead isotope evolution by a two-stage model. Earth Planet. Sci. Lett. 26, 207–221.

Stern T. W., Goldich S. S., Newel M. F. (1966): Effect of weathering on the U-Pb zircon ages from the Morton gneiss, Minnesota. Earth Planet. Sci. Lett. 1, 369–378.

Tchameni R. (1997): Géochimie et géochronologie des formations de l'Archéen et du Paléoproterozoï que du Sud-Cameroun (Groupe du Ntem, Craton du Congo). Thèse de l'Univérsité d'Orléans, France.

Tchameni R., Mezger K., Nsifa N. E., Pouclet A. (2000): Neoarchaean evolution in the Congo Craton: evidence from K rich granitoids of the Ntem complex, Southern Cameroon. J. Afr. Earth Sci. 30, 133–147.

Tchameni R., Mezger K., Nsifa N. E., Pouclet A. (2001): Crustal origin of Early Proterozoic syenites in the Congo craton (Ntem complex), South Cameroon. Lithos 57, 23–42.

Toteu S. M., Van Schmus W. R., Penaye J., Nyobe J. B. (1994): U-Pb and Sm-Nd evidence for Eburnean and Pan-African high grade metamorphism in cratonic rocks of Southern Cameroon. Precambrian Res. 67, 321–347.

Vavra G. (1990): On the kinematics of zircon growth and its petrogenetic significance: a cathodoluminescence study. Contrib. Mineral. Petrol. 106, 90–99.

Vavra G. (1994): Systematics of internal zircon morphology in major Variscan granitoid types. Contrib. Mineral. Petrol. 117, 331–344.

Vavra G., Gebauer D., Schmid R., Compston W. (1996): Multiple zircon growth and recrystallization during polyphase late Carboniferous to Triassic metamorphism in granulites of the Ivrea Zone (Southern Alps): an ion microprobe (SHRIMP) study. Contrib. Mineral. Petrol. 122, 337–358.

Vavra G., Schmid R., Gebauer D. (1999): Internal morphology, habit and U-Th-Pb microanalysis of amphibole to granulite facies zircon. Contrib. Mineral. Petrol. 134, 380–404.

Verwoerd W. J. (1986): Mineral deposits associated with carbonatites and alkaline rocks. In: Anhaeusser C. R., Maske S. (eds) Mineral deposits of Southern Africa, II. Geol. Soc. S. Afr., Johannesburg, 2173–2191.

Vicat J. P., Leger J. M., Nsifa E., Piguet P., Nzenti J. P., Tchameni R., Pouclet A. (1996): Distinction au sein du craton congolais du Sud-Ouest du Cameroun, de deux épisodes doléritiques initiant les cycles orogéniques éburnéen (Paléoprotérozoï que) et Pan-Africain (Néoprotérozoï que). C. R. Acad. Sci. Paris, 323, série IIa, 575–582.

Wasserburg D. J. (1963): Diffusion processes in lead-uranium systems. J. Geophys. Res. 68, 4823–4846.

Wetherill G. S. (1956): Discordant uranium-lead ages. I. Trans. Am. Geophys. Union 37, 320–326.

Wendt I. (1984): A three dimensional U-Pb discordia plane to evaluate samples with common lead of unknown isotopic composition. Isot. Geosci. 2, 1–12.

Wendt I. (1986): Radiometrische Methoden in der Geochronologie. Clausthaler Tektonische Hefte 23, Pilger Verlag.

Whitehouse M. J., Kamber B. S., Moorbath S. (1999): Age significance of U-Th-Pb zircon data from early Archaean rocks of west Greenland – a reassessment based on combined ion-probe and imaging studies. Chem. Geol. 160, 201–224.

Wiedenbeck M., Alle P., Corfu F., Griffin W. L., Meier M., Oberli F., Von Quadt A., Roddick J. C., Spiegel W. (1995): Three natural zircon standards for U-Th-Pb, Lu-Hf, trace element and REE analyses. Geostand. Newsl. 19, 1–23.